

Spectral domain optical coherence tomography cross-sectional image of optic nerve head during intraocular pressure elevation

Ji Young Lee, You Kyung Lee, Jung Il Moon, Myoung Hee Park

Department of Ophthalmology, Yeouido St. Mary's Hospital, College of Medicine, the Catholic University of Korea, 62, Yeuido-dong, Youngdeungpo-gu, Seoul 150-713, Korea

Correspondence to: Myoung Hee Park. Department of Ophthalmology, Yeouido St. Mary's Hospital, College of Medicine, The Catholic University of Korea, 62, Yeuido-dong, Youngdeungpo-gu, Seoul 150-713, Korea. marypark@catholic.ac.kr

Received: 2013-09-04

Accepted: 2013-12-12

Abstract

• **AIM:** To analyze changes of the optic nerve head (ONH) and peripapillary region during intraocular pressure (IOP) elevation in patients using spectral domain optical coherence tomography (SD-OCT).

• **METHODS:** Both an optic disc 200×200 cube scan and a high-definition 5-line raster scan were obtained from open angle glaucoma patients presented with monocular elevation of IOP (≥ 30 mm Hg) using SD-OCT. Additional baseline characteristics included age, gender, diagnosis, best-corrected visual acuity, refractive error, findings of slit lamp biomicroscopy, findings of dilated stereoscopic examination of the ONH and fundus, IOP, pachymetry findings, and the results of visual field.

• **RESULTS:** The 24 patients were selected and divided into two groups: group 1 patients had no history of IOP elevation or glaucoma ($n=14$), and group 2 patients did have history of IOP elevation or glaucoma ($n=10$). In each patient, the study eye with elevated IOP was classified into group H (high), and the fellow eye was classified into group L (low). The mean deviation (MD) differed significantly between groups H and L when all eyes were considered ($P=0.047$) and in group 2 ($P=0.042$), not in group 1 ($P=0.893$). Retinal nerve fiber layer (RNFL) average thickness ($P=0.050$), rim area ($P=0.015$), vertical cup/disc ratio ($P=0.011$), cup volume ($P=0.028$), inferior quadrant RNFL thickness ($P=0.017$), and clock-hour (1, 5, and 6) RNFL thicknesses ($P=0.050$, 0.012, and 0.018, respectively), cup depth ($P=0.008$), central prelaminar layer thickness ($P=0.023$), mid-inferior prelaminar layer thickness ($P=0.023$), and nasal retinal slope ($P=0.034$) were significantly different between the eyes with groups H and L.

• **CONCLUSION:** RNFL average thickness, rim area, vertical cup/disc ratio, cup volume, inferior quadrant RNFL thickness, and clock-hour (1, 5, and 6) RNFL thicknesses significantly changed during acute IOP elevation.

• **KEYWORDS:** spectral domain optical coherence tomography; optic nerve head; elevated intraocular pressure; open angle glaucoma; retinal nerve fiber layer

DOI: 10.3980/j.issn.2222-3959.2014.06.21

Lee JY, Lee YK, Moon JI, Park MH. Spectral domain optical coherence tomography cross-sectional image of optic nerve head during intraocular pressure elevation. *Int J Ophthalmol* 2014;7(6):1022-1029

INTRODUCTION

Glaucoma is a neurodegenerative disease of the optic nerve characterized by the accelerated death of retinal ganglion cells (RGCs) and their axons. The death of RGCs ultimately leads to progressive visual field loss and eventual blindness^[1]. Elevated intraocular pressure (IOP) is the most important risk factor for glaucomatous optic neuropathy^[2-4]. According to the recently suggested biomechanical paradigm, IOP plays a central role in the pathogenesis of optic nerve damage in glaucoma^[5]. There is mounting evidence to suggest that the primary site of injury to the retinal ganglion cell axon is at the level of the lamina cribrosa (LC) by elevated IOP^[6-10]. Elevated IOP causes posterior and lateral displacement of the LC of the optic nerve head (ONH)^[11,12]. This may generate strain on the optic nerve. The resulting tensile strain within the LC would provide shearing stress on the axons passing through the laminar pores. And the LC deformation may be relevant with optic nerve ischemia because the strain within the LC can compress the laminar capillaries, which are contained in the laminar trabeculae^[1]. In addition, clinical studies have suggested that microcirculatory changes may have a role in glaucoma. Elevated IOP is caused by the abnormal outflow of aqueous humor through the trabecular meshwork (TM), a meshwork of connective tissue lining the outflow pathway at the iridocorneal angle of the anterior chamber of the eye^[13,14]. Furthermore, the relevance of oxidative stress to the pathogenesis of glaucoma has been demonstrated in cell and animal studies. Elevated IOP causes oxidative stress in the

extracellular matrix of the TM, which in turn increases IOP and leads to apoptosis of RGCs^[15-17].

Recently, several studies have used spectral domain optical coherence tomography (SD-OCT) to visualize the ONH^[18-21]. Lee *et al*^[19] showed *in vivo* images of backward bowing of the human ONH using the enhanced depth-imaging technique of SD-OCT. Na *et al*^[20] revealed that measurement of ONH, retinal nerve fiber layer (RNFL) and macular parameters using SD-OCT identified progression in glaucomatous eyes. Park *et al*^[21] revealed that the LC was thinner in a normal-tension glaucoma patient than in patients with high-pressure open-angle glaucoma; this implies that the LC is more vulnerable to glaucomatous damage in normal-tension glaucoma than in high-pressure open-angle glaucoma under the same pressure, emphasizing again the importance of the LC in the pathogenesis of glaucoma.

Furthermore, recent work using postmortem three dimensional histomorphometric ONH reconstructions has identified several cardinal morphologic changes at the earliest stage of experimental glaucoma^[22-26]. These changes include increasing cup volume and thickening of the prelaminar tissue.

To our knowledge, no SD-OCT study has shown changes of the peripapillary retina and ONH during a period of IOP elevation *in vivo*. In this study, we analyzed changes of the ONH and peripapillary region during IOP elevation in patients with monocular IOP elevation, using SD-OCT.

SUBJECTS AND METHODS

This study was approved by the Yeouido St. Mary's Hospital Institutional Review Board, the Catholic University of Korea, Seoul, Korea (Subject Number SC12RISI0037). All study proceedings were in accordance with the principles of the Declaration of Helsinki. Informed consent was obtained from all patients enrolled in the study. We retrospectively reviewed the medical records of 24 patients who received both 200×200 cube scans and high-definition 5-line raster scans of the ONH by SD-OCT (Cirrus OCT; Carl Zeiss-Meditec, Inc., Dublin, CA, USA) in Yeouido St. Mary's Hospital Glaucoma Clinic from March 2011 to February 2012. Since the purchase of the SD-OCT instrument in December 2010, a 200×200 cube scan and high-definition 5-line raster scan of the ONH have been performed in series for all patients needing SD-OCT for initial diagnosis or follow-up of glaucomatous optic neuropathy. Subjects were imaged through undilated pupils. First, a 200×200 cube scan was obtained at the central optic disc, followed by a 5-line high-definition raster scan at the same location. The slice length (6.00 mm) and spacing distance (0.25 mm) were determined automatically by the machine.

The inclusion criteria for patients were: diagnosis of monocular elevation of IOP (≥ 30 mm Hg), with a Goldmann applanation tonometer reading performed on the same day as

SD-OCT; diagnosis of open-angle glaucoma by gonioscopy; the presence of a clinically open angle (angle of the anterior chamber) and significant cupping of the optic disc (>0.7); typical reproducible visual field changes, viz. arcuate, Bjerrum, Seidel, paracentral and annular scotoma and nasal steps; ocular medium clear enough to allow visualization of the ONH and macula; and signal strength ≥ 6 on examined SD-OCT 200×200 cube scan and corresponding 5-line raster scan of the ONH. We excluded patients who were diagnosed with bilateral IOP elevation, bilateral glaucoma, ocular hypertension or acute angle-closure glaucoma; had IOP <30 mm Hg at the time of SD-OCT; had poor visualization of the ONH due to ocular medium opacity; had signal strength <6 on SD-OCT scan images; had optic neuropathy other than glaucoma; or were highly myopic (<-8 diopters by spherical equivalent). The following data were collected for each patient: age, gender, diagnosis, best-corrected visual acuity, refractive error, findings of slit lamp biomicroscopy, findings of dilated stereoscopic examination of the ONH and fundus, IOP determined by Goldmann applanation tonometry, pachymetry findings, and the results of achromatic automated perimetry using a 24-2 Swedish Interactive Threshold Algorithm (SITA) standard program (Humphrey visual field analyzer; Carl Zeiss-Meditec, Inc.).

From the RNFL and ONH analyses of the 200×200 optic disc cube scans, the average RNFL thickness, RNFL symmetry, rim area, disc area, average cup/disc (C/D) ratio, vertical C/D ratio, cup volume, values of the RNFL quadrants map, and values of the RNFL clock hours map were determined for each eye. The cup depth, prelaminar layer thickness, and retinal margin slope were measured from the third cross-sectional B-scan images (middle portion) of the high-definition 5-line raster scans of the ONH (Figure 1A). A line connecting both ends of Bruch's membrane is used as the reference line (Figure 1B, x). Another line is drawn perpendicular to this reference line at the point of the deeper most region of the optic disc cup (Figure 1B, y). Cup depth was defined as the distance from the line connecting each end of the Bruch's membrane (x) to the deepest portion of the optic disc cup in the central cross-sectional image of each eye (Figure 1B, b, long double arrow). Prelaminar layer thickness was defined as the length from the anterior border of the LC (Figure 1B, short double arrow), which appears as a highly reflective region (Figure 1B, arrow heads) at the vertical center of the ONH in horizontal SD-OCT cross-sectional B-scan image. Because the thick central retinal vessels produce posterior shadowing in cross-sectional B-scans, prelaminar thickness was measured at the temporal side of the trunk of the central retinal vessels. To compare the regional variation of the prelaminar layer thickness, measurements were also made at the second and fourth cross-sectional B-scan images of the

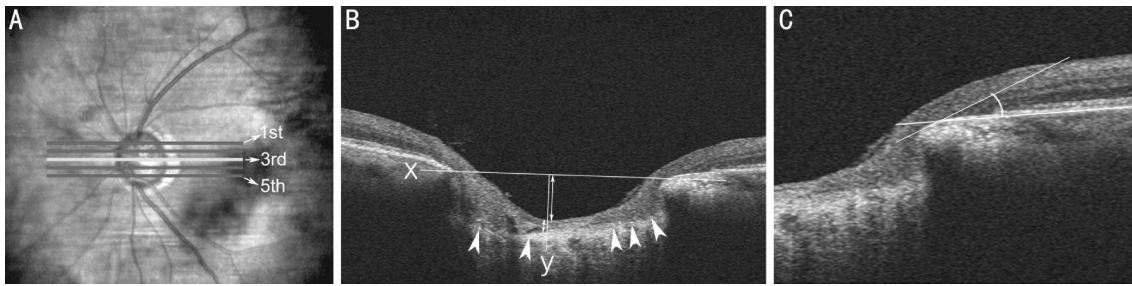


Figure 1 RNFL and ONH imaging using SD-OCT A: OCT scan image of optic disc head; B: Cross-sectional image obtained in 3rd scan; C: Magnified view of retinal margin obtained in 3rd scan.

high-definition 5-line raster scan. Retinal slope was defined as the angle between Bruch's membrane and posterior border of RNFL (Figure 1C).

Cup depth and prelaminar layer thickness were measured using Cirrus high-definition (HD)-OCT software. However, Cirrus HD-OCT software does not provide an angle measurement tool; thus, image software (National Institutes of Health; available at: <http://rsbweb.nih.gov/ij/>; accessed December 20, 2009) was used to measure the retinal margin slopes at the temporal and nasal sites of the ONH in each eye. By a previously reported method, the raw cross-sectional B-scan image data from Cirrus HD-OCT was converted to match the real pixel ratio (1:3, horizontal: vertical ratio), and the units were converted to micrometers [27]. Retinal slope was defined as the angle between Bruch's membrane and posterior border of RNFL. The angle between Bruch's membrane and posterior border of RNFL was measured (Figure 1C). All measurements were performed by one author (Park MH).

The patients were divided into two groups. Group 1 patients were those with no history of IOP elevation or glaucoma. Group 2 patients had a history of glaucoma. In each patient, the study eye with elevated IOP was categorized into group H (high). The IOP in the fellow eye was controlled at <22 mm Hg, by either medication or surgery, and this eye was categorized into group L (low).

Statistical analyses were performed using SPSS software (version 19.0.0; SPSS, Inc., Chicago, IL, USA). Wilcoxon signed-rank test was used to compare data between group H and group L. Mann-Whitney U test was used to compare data between group 1 and group 2. The level of statistical significance was defined as $P < 0.05$.

RESULTS

Among the 377 patients who underwent both an optic disc 200×200 cube scan and a high-definition 5-line raster scan from March 2011 to February 2012, 41 patients had an IOP >30 mm Hg the day of the SD-OCT measurement. 17 patients were excluded because of bilateral disease ($n=6$), low signal strength (<6) of SD-OCT images ($n=3$), or acute attack of angle-closure glaucoma ($n=8$). The remaining 24 patients were divided into two groups: group 1 patients had no

history of IOP elevation or glaucoma ($n=14$), and group 2 patients did have history of IOP elevation or glaucoma ($n=10$). In each patient, the study eye with elevated IOP was classified into group H, and the normal fellow eye with IOP <22 mm Hg was classified into group L.

The basic demographic factors are shown in Table 1. Group 2 eyes had a thicker central cornea in both the eye with high IOP ($P=0.025$) and the eye with low IOP ($P=0.037$). IOP was significantly higher in group H eyes compared with group L eyes ($P=0.002$), and the eyes with higher IOP had greater myopic refractive error ($P=0.005$). The mean deviation (MD) of the Humphrey visual field test differed significantly between the group H and group L when all eyes were considered ($P=0.047$) and in group 2. However, the MD was not significantly different between the group H and group L eyes in group 1 ($P=0.893$). When comparing group 1 with group 2, the MD for group H eyes were significantly different ($P=0.009$), whereas the MD for group L eyes did not differ significantly between the group 1 and group 2 ($P=0.075$).

The results of the ONH and RNFL analyses based on the 200×200 optic disc cube scans are presented in Tables 2, 3. Considering all eyes, RNFL average thickness ($P=0.050$), rim area ($P=0.015$), vertical cup/disc ratio ($P=0.011$), cup volume ($P=0.028$), inferior quadrant RNFL thickness ($P=0.017$), and clock-hour (1, 5, and 6) RNFL thicknesses ($P=0.050$, 0.012, and 0.018, respectively) were significantly different between the eyes with elevated IOP (group H) and the normal fellow eyes (group L). None of these parameters differed significantly between the group H and group L eyes within group 1, and only some parameters showed a significant difference within group 2.

Table 4 describes the analysis results of the morphological factors on ONH cross-sectional images. Considering all eyes, cup depth ($P=0.008$), central prelaminar layer thickness ($P=0.023$), mid-inferior prelaminar layer thickness ($P=0.023$), and nasal retinal slope ($P=0.034$) were significantly different between eyes with elevated IOP (group H) and normal fellow eyes (group L). When the analysis was performed separately for group 1 and group 2, cup depth in group 2 was significantly different between eyes with elevated IOP (group H) and normal fellow eyes (group L).

Table 1 Patient characteristics of each group

Characteristics	Total (n=24)	Group 1 (n=14)	Group 2 (n=10)	¹ P
Age (a)	56.50±14.89	57.71±10.90	54.80±20.62	0.744
Spherical equivalent of refractive error (diopters)				
H	-2.67±1.91	-3.13±2.08	-2.65±4.00	0.784
L	-1.66±2.87	-1.92±2.50	-1.35±3.54	0.464
² P	0.005	0.042	0.041	NA
Central corneal thickness (µm)				
H	565.78±21.52	551.40±12.84	583.75±15.48	0.014
L	571.00±22.61	554.00±15.60	588.00±13.39	0.021
² P	0.310	0.593	0.465	NA
IOP (mm Hg)				
H	40.50±8.17	39.71±8.71	41.60±8.20	0.807
L	17.17±3.49	17.71±3.45	16.40±3.78	0.188
² P	0.002	0.018	0.042	NA
MD (dB)				
H	-11.09±11.79	-2.37±2.12	-19.80±10.64	0.009
L	-2.66±1.63	-2.07±1.61	-2.15±1.58	0.175
² P	0.047	0.893	0.043	NA
PSD (dB)				
H	0.73±0.78	0.88±0.81	0.29±0.64	0.166
L	0.94±0.66	0.91±0.71	0.79±0.73	0.459
² P	0.893	0.715	0.285	NA

Group 1: Patients with no history of IOP elevation or glaucoma; Group 2: Patients with history of IOP elevation or glaucoma; H: Eyes with elevated IOP; L: Fellow eyes with normal IOP; MD: Mean deviation of the Humphrey visual field test; PSD: Pattern standard deviation of the Humphrey visual field test; NA: Not applicable. ¹Wilcoxon signed-rank test; ²Mann-Whitney U test.

DISCUSSION

In the present study, average RNFL thickness, rim area, vertical cup/disc ratio, cup volume, inferior quadrant RNFL thickness, and vertical clock-hour RNFL thicknesses [1/11 (superonasal), 5/7 (inferonasal), and 6] were significantly different between the group H and group L (Tables 2, 3). These parameters were more significant difference when the analysis was performed by combining groups 1 and 2 than when group 2 was analyzed separately, even though group 2 was composed of eyes with past glaucomatous optic neuropathy. Some of these findings are in agreement with other studies. Mwanza *et al*^[27] demonstrated that vertical rim thickness, rim area, RNFL thickness at clock hour 7/5 (interotemporal), inferior quadrant RNFL thickness, vertical cup/disc ratio, and average RNFL thickness were valuable in distinguishing normal conditions from glaucoma, regardless of the disease stage. Regional anatomical differences of the lamina (larger pores in the superior and inferior areas of the LC) have been cited as reasons for these characteristic vertical rim and RNFL changes in glaucomatous optic neuropathy^[28].

Cup depth, central prelaminar layer thickness, mid-inferior prelaminar layer thickness, and nasal retinal slope were also significant difference between the group H and group L. These findings were consistent with result of Yang *et al*^[23];

deep cupping and thickened prelaminar tissue in monkey with early experimental glaucoma. Thickening of prelaminar layer thickness in the central and mid-inferior regions of the optic disc may be associated with changes in the peripapillary RNFL thickness in the inferior quadrant. Because our data includes eyes with previously diagnosed glaucoma, it is unclear whether changes in the RNFL thickness occur immediately after IOP elevation or develop later. Further studies are needed to determine why inferior regions of the prelaminar layer and RNFL are more vulnerable to IOP elevation than superior regions.

Our study also revealed that the peripapillary retinal slope was flatter in IOP elevation group without history of IOP elevation than with previous glaucoma optic neuropathy. Manjunath *et al*^[29] performed an analysis of the peripapillary atrophy area using SD-OCT and demonstrated abnormal retinal sloping in patients with glaucoma. Normal eyes had a 90-degree angle between the optic disc edge and retinal pigment epithelium, whereas eyes with glaucoma had less retinal sloping. Hayashi *et al*^[30] reported a positive relationship between glaucomatous eyes and the downward-curved appearance of Bruch's membrane, which was not seen in simple myopic changes. In the present study, the nasal peripapillary retinal slope was significantly flatter in the eyes with elevated IOP than in the normal fellow eyes.

Structure change during intraocular pressure elevation

Table 2 ONH analysis from optic disc cube 200×200 scan of each group

Parameters	Total (n=24)	Group 1 (n=14)	Group 2 (n=10)	¹ P
Rim area (mm ²)				
H	0.72±0.29	0.90±0.19	0.57±0.28	0.049
L	1.17±0.25	1.26±0.37	1.11±0.12	1.000
² P	0.015	0.273	0.043	NA
Disc area				
H	1.87±0.40	1.65±0.55	2.04±0.10	0.221
L	1.82±0.33	1.71±0.50	1.91±0.07	0.806
² P	0.374	0.715	0.043	NA
Average cup/disc ratio				
H	0.74±0.15	0.61±0.14	0.84±0.07	0.019
L	0.62±0.18	0.60±0.28	0.64±0.05	0.624
² P	0.097	1.000	0.068	NA
Vertical cup/disc ratio				
H	0.72±0.16	0.59±0.11	0.83±0.09	0.014
L	0.62±0.18	0.50±0.18	0.64±0.52	0.327
² P	0.011	0.144	0.042	NA
Cup volume				
H	0.44±0.29	0.23±0.18	0.70±0.14	0.034
L	0.23±0.14	0.16±0.12	0.31±0.14	0.157
² P	0.028	0.144	0.109	

Group 1: Patients with no history of IOP elevation or glaucoma; Group 2: Patients with history of IOP elevation or glaucoma; RNFL: Retinal nerve fiber layer; H: Eyes with elevated IOP; L: Fellow eyes with normal IOP; NA: Not applicable. ¹Wilcoxon signed-rank test; ²Mann-Whitney U test.

Table 3 RNFL thickness analysis from optic disc cube 200×200 scan of each group

Parameters	Total (n=24)	Group 1 (n=14)	Group 2 (n=10)	¹ P
Average RNFL thickness (µm)				
H	80.98±16.01	93.15±8.75	68.80±11.39	0.016
L	91.10±9.06	96.41±8.60	85.80±6.34	0.075
² P	0.050	0.465	0.068	NA
Superior quadrant RNFL thickness				
H	86.50±19.72	103.67±15.95	76.20±14.13	0.053
L	106.00±10.30	101.67±11.68	108.60±9.74	0.453
² P	0.069	0.285	0.043	NA
Inferior quadrant RNFL thickness				
H	87.00±19.24	97.33±21.36	80.80±17.06	0.180
L	115.38±7.31	118.33±7.51	113.60±7.40	0.653
² P	0.017	0.285	0.043	NA
Temporal quadrant RNFL thickness				
H	65.50±20.15	83.67±16.29	54.60±13.48	0.053
L	66.38±16.54	77.67±5.03	59.60±12.18	0.180
² P	0.779	0.109	0.686	NA
Nasal quadrant RNFL thickness				
H	82.00±67.88	75.33±7.02	63.40±4.98	0.053
L	65.75±5.04	64.67±5.03	66.40±5.50	0.546
² P	0.612	0.109	0.068	NA

Group 1: Patients with no history of IOP elevation or glaucoma; Group 2: Patients with history of IOP elevation or glaucoma; RNFL: Retinal nerve fiber layer; H: Eyes with elevated IOP; L: Fellow eyes with normal IOP; NA: Not applicable. ¹Wilcoxon signed-rank test; ²Mann-Whitney U test.

The mean temporal slope was also flatter in the eyes with elevated IOP, but this was not statistically significant. It

appears that the pressure gradient during IOP elevation pushes the peripapillary retina and Bruch's membrane

Table 3 RNFL thickness analysis from optic disc cube 200×200 scan of each group (continued)

Clock-hour RNFL thickness (R/L)	Total (n=24)	Group 1 (n=14)	Group 2 (n=10)	¹ P	Clock-hour RNFL thickness (R/L)	Total (n=24)	Group 1 (n=14)	Group 2 (n=10)	¹ P
12					6				
H	84.50±28.17	94.00±37.75	78.80±23.83	0.655	H	86.63±16.98	96.33±14.57	80.80±16.89	0.180
L	105.25±22.29	91.00±29.87	113.80±13.41	0.230	L	122.50±17.95	117.67±19.43	125.40±18.64	0.456
² P	0.123	0.593	0.080	NA	² P	0.018	0.180	0.043	NA
1/11					7/5				
H	83.25±22.77	104.33±22.50	70.60±10.99	0.053	H	110.00±35.61	138.33±18.58	93.00±32.91	0.101
L	115.63±17.86	117.00±24.27	114.80±16.18	0.881	L	91.63 12.61	88.67±10.79	93.40±14.48	0.456
² P	0.050	0.593	0.043	NA	² P	0.176	0.109	1.000	NA
2/10					8/4				
H	78.25±16.02	93.67±8.74	69.00±11.20	0.051	H	68.38±18.24	85.67±22.01	57.60±20.17	0.099
L	79.00±21.57	93.67±29.02	70.20±11.63	0.294	L	61.38±7.21	58.67±5.13	63.00±8.31	0.297
² P	0.833	1.000	0.686	NA	² P	0.575	0.109	0.345	NA
3/9					9/3				
H	63.00±10.06	69.67±9.50	59.00±8.86	0.101	H	52.75±15.67	62.67±20.50	46.80±10.08	0.230
L	54.38±14.64	64.00±14.00	48.60±12.88	0.131	L	58.50±5.66	57.00±6.25	59.40±5.81	0.456
² P	0.128	0.593	0.144	NA	² P	0.206	0.593	0.080	NA
4/8					10/2				
H	62.38±5.48	63.00±7.21	62.00±5.10	0.881	H	68.38±18.24	84.00±12.29	59.00±14.63	0.053
L	66.13±17.88	75.33±16.80	60.60±17.78	0.180	L	77.00±10.41	77.00±14.73	77.00±9.00	0.881
² P	0.735	0.180	0.893	NA	² P	0.208	0.285	0.080	NA
5/7					11/1				
H	70.75±10.21	75.33±14.19	68.00±7.52	0.297	H	91.25±22.29	112.33±15.04	78.60±14.93	0.053
L	131.13±19.03	147.00±10.00	121.60±16.77	0.053	L	97.13±16.41	98.00±24.06	96.60±13.45	0.881
² P	0.012	0.109	0.043	NA	² P	0.440	0.593	0.080	NA

Group 1: Patients with no history of IOP elevation or glaucoma; Group 2: Patients with history of IOP elevation or glaucoma; RNFL: Retinal nerve fiber layer; H: Eyes with elevated IOP; L: Fellow eyes with normal IOP; NA: Not applicable. ¹Wilcoxon signed-rank test; ²Mann-Whitney U test.

complex; the contour may change more easily because of the structural heterogeneity around the ONH. In most eyes, the slope of the retinal margin was flatter in the temporal region of the optic disc head than in the nasal region. At the same IOP, a steeper area (nasal retinal margin) is more vulnerable to change than a flatter area (temporal retinal margin) because it receives a larger pressure gradient. This may explain why the retinal rim slope change was significant only in the nasal margin. Considering all of these findings, it seems certain that flattening of the peripapillary retinal slope occurs by IOP elevation.

OCT can produce high-resolution *in vivo* cross-sectional images of the ONH, retina, and choroid. However, because OCT uses a super-luminescent diode laser beam, the image quality is easily affected by the medium opacity such as that caused by corneal opacity or cataracts. Thus, patients with an acute attack of angle closure are not generally suitable candidates for OCT because their condition is almost always accompanied by corneal edema. Patients with secondary open angle glaucoma, such as glaucomatocyclitic crisis, usually demonstrate clear ocular medium, allowing imaging of the ONH with good signal strength.

A limitation of our study was that we used Cirrus OCT without enhanced depth-imaging and thus could not observe the whole thickness of the LC. We measured only the prelaminar layer thickness from the anterior border of the lamina to the surface of the prelaminar nerve fiber layer near the trunk of the central retinal vessels. The prelaminar layer thicknesses measured in this study appeared to be different from previously reported values. Measurements may vary according to the measuring device and the observer, making direct comparisons of results among different studies meaningless. Nevertheless, our study results showed differences in the central prelaminar thickness between the eyes with elevated IOP and normal fellow eyes. The prelaminar thickness measured by Lee *et al* [19] was not significantly different among normal subjects (111.43±34.98, *n*=10), glaucoma suspects (93.83±18.74, *n*=7), and glaucoma patients (95.70±18.46, *n*=18), although the laminar thickness was significantly different among the three groups. Further evaluation is needed to determine whether there is a difference in the response to acute IOP elevation between the prelaminar and laminar layers. Our study was cross-sectional study, observed only during elevation IOP. As a cross-sectional study, our data was collected during the IOP was

Table 4 Analysis results of morphological factors on ONH cross-sectional images

Parameters	Total (n=24)	Group 1 (n=14)	Group 2 (n=10)	¹ P
Cup depth (μm)				
H	314.89±211.84	193.86±172.97	484.34±130.44	0.019
L	189.62±140.32	112.31±99.49	297.86±119.16	0.019
² P	0.008	0.116	0.043	NA
Central prelaminar layer thickness (μm)				
H	126.15±53.25	117.46±24.12	138.32±81.29	0.745
L	204.72±118.53	203.34±109.43	206.66±143.87	0.935
² P	0.023	0.128	0.080	NA
Mid-superior prelaminar layer thickness (μm)				
H	153.88±74.42	160.41±67.91	144.08±93.36	0.831
L	154.14±136.97	139.33±136.39	174.89±150.89	0.806
² P	0.878	0.917	0.715	NA
Mid-inferior prelaminar layer thickness (μm)				
H	175.29±100.03	186.78±118.94	159.20±75.77	0.808
L	327.45±178.11	317.87±180.43	340.87±194.98	0.935
² P	0.023	0.128	0.080	NA
Temporal retinal rim slope (degree)				
H	34.38±13.93	39.15±15.70	27.71±8.26	0.167
L	42.26±20.28	43.61±26.59	40.35±7.92	0.465
² P	0.209	0.735	0.138	NA
Nasal retinal rim slope (degree)				
H	35.68±19.20	39.25±20.78	30.69±17.66	0.570
L	55.17±16.63	57.62±18.51	51.75±14.88	0.570
² P	0.034	0.128	0.138	NA

Group 1: Patients with no history of IOP elevation or glaucoma; Group 2: Patients with history of IOP elevation or glaucoma; H: Eyes with elevated IOP; L: Fellow eyes with normal IOP; NA: Not applicable. ¹Wilcoxon signed-rank test; ²Mann-Whitney U test.

high, therefore, further investigation is required to obtain serial data of ONH and RNFL parameters after lowering IOP and compare them with values of elevated IOP.

Despite the limitations of Cirrus OCT without enhanced depth-imaging for visualizing the LC, we obtained clear images of the choroidal vascular beds around the optic disc. Compared with a 200 × 200 cube scan, a high-definition 5-line raster scan has a shorter scanning time and thus has less artifact motion from eye movement or blinking, resulting in a more detailed cross-sectional image of the ONH and peripapillary region. As the ONH diameter is about the same span as the 5-line raster scan area in the majority of patients, the first and fifth scan image can visualize the upper and lower ends of the ONH, respectively, and the third scan image usually shows the central portion of the ONH (Figure 1). In conclusion, using SD-OCT, we observed morphology of the ONH and peripapillary area during IOP elevation. RNFL average thickness, rim area, vertical cup/disc ratio, cup volume, inferior quadrant RNFL thickness, and clock-hour (1, 5, and 6) RNFL thicknesses were more significantly changed during IOP elevation without history of IOP elevation than with history of IOP elevation.

ACKNOWLEDGEMENTS

Conflicts of Interest: Lee JY, None; Lee YK, None; Moon JI, None; Park MH, None.

REFERENCES

- Howell GR, Libby RT, Jakobs TC, Smith RS, Phalan FC, Barter JW, Barbay JM, Marchant JK, Mahesh N, Porciatti V, Whitmore AV, Masland RH, John SW. Axons of retinal ganglion cells are insulated in the optic nerve early in DBA/2J glaucoma. *J Cell Biol* 2007;179(7):1523–1537
- McMonnies CW. Intraocular pressure spikes in keratectasia, axial myopia, and glaucoma. *Optom Vis Sci* 2008;85(10):1018–1026
- Crichton A, Drance SM, Douglas GR, Schulzer M. Unequal intraocular pressure and its relation to asymmetric visual field defects in low-tension glaucoma. *Ophthalmology* 1989;96(9):1312–1314
- Abedin S, Simmons RJ, Grant WM. Progressive low-tension glaucoma: treatment to stop glaucomatous cupping and field loss when these progress despite normal intraocular pressure. *Ophthalmology* 1982;89(1):1–6
- Burgoyne CF, Downs JC, Bellezza AJ, Suh JK, Hart RT. The optic nerve head as a biomechanical structure: a new paradigm for understanding the role of IOP-related stress and strain in the pathophysiology of glaucomatous optic nerve head damage. *Prog Retin Eye Res* 2005;24(1):39–73
- Gaasterland D, Tanishima T, Kuwabara T. Axoplasmic flow during chronic experimental glaucoma: 1. light and electron microscopic studies of the monkey optic nerve head during development of glaucomatous cupping. *Invest Ophthalmol Vis Sci* 1978;17(9):838–846
- Minckler DS, Bunt AH, Johanson GW. Orthograde and retrograde

- axoplasmic transport during acute ocular hypertension in the monkey. *Invest Ophthalmol Vis Sci* 1977;16(5):426-441
- 8 Quigley HA, Green WR. The histology of human glaucoma cupping and optic nerve damage: clinicopathologic correlation in 21 eyes. *Ophthalmology* 1979;86(10):1803-1830
- 9 Quigley HA, Addicks EM, Green WR, Maumenee AE. Optic nerve damage in human glaucoma. II: The site of injury and susceptibility to damage. *Arch Ophthalmol* 1981;99(4):635-649
- 10 Bellezza AJ, Rintalan CJ, Thompson HW, Downs JC, Hart RT, Burgoyne CF. Deformation of the lamina cribrosa and anterior scleral canal wall in early experimental glaucoma. *Invest Ophthalmol Vis Sci* 2003;44 (2): 623-637
- 11 Burgoyne CF, Downs JC, Bellezza AJ, Hart RT. Three-dimensional reconstruction of normal and early glaucoma monkey optic nerve head connective tissues. *Invest Ophthalmol Vis Sci* 2004;45(12):4388-4399
- 12 Quigley HA, Addicks EM. Chronic experimental glaucoma in primates. II. Effect of extended intraocular pressure elevation on optic nerve head and axonal transport. *Invest Ophthalmol Vis Sci* 1980;19(2):137-152
- 13 Loewen N, Fautsch MP, Peretz M, Bahler CK, Cameron JD, Johnson DH, Poeschla EM. Genetic modification of human trabecular meshwork with lentiviral vectors. *Hum Gene Ther* 2001;12(17): 2109-2119
- 14 Zhang M, Maddala R, Rao PV. Novel molecular insights into RhoA GTPase-induced resistance to aqueous humor outflow through the trabecular meshwork. *Am J Physiol Cell Physiol* 2008;295(5):C1057-1070
- 15 Saccà SC, Izzotti A. Oxidative stress and glaucoma: injury in the anterior segment of the eye. *Prog Brain Res* 2008;173:385-407
- 16 Bagnis A, Izzotti A, Centofanti M, Saccà SC. Aqueous humor oxidative stress proteomic levels in primary open angle glaucoma. *Exp Eye Res* 2012;103:55-62
- 17 Izzotti A, Saccà SC, Longobardi M, Cartiglia C. Sensitivity of ocular anterior chamber tissues to oxidative damage and its relevance to the pathogenesis of glaucoma. *Invest Ophthalmol Vis Sci* 2009;50 (11): 5251-5258
- 18 Kagemann L, Ishikawa H, Wollstein G, Brennen PM, Townsend KA, Gabriele ML, Schuman JS. Ultrahigh-resolution spectral domain optical coherence tomography imaging of the lamina cribrosa. *Ophthalmic Surg Lasers Imaging* 2008;39(4 Suppl):S126-131
- 19 Lee EJ, Kim TW, Weinreb RN, Park KH, Kim SH, Kim DM. Visualization of the lamina cribrosa using enhanced depth imaging spectral-domain optical coherence tomography. *Am J Ophthalmol* 2011; 152(1):87-95
- 20 Na JH, Sung KR, Lee JR, Lee KS, Baek S, Kim HK, Sohn YH. Detection of glaucomatous progression by spectral-domain optical coherence tomography. *Ophthalmology* 2013;120(7):1388-1395
- 21 Park HY, Jeon SH, Park CK. Enhanced depth imaging detects lamina cribrosa thickness differences in normal tension glaucoma and primary open-angle glaucoma. *Ophthalmology* 2012;119(1):10-20
- 22 Roberts MD, Grau V, Grimm J, Reynaud J, Bellezza AJ, Burgoyne CF, Downs JC. Remodeling of the connective tissue microarchitecture of the lamina cribrosa in early experimental glaucoma. *Invest Ophthalmol Vis Sci* 2009;50(2):681-690
- 23 Yang H, Downs JC, Bellezza AJ, Thompson H, Burgoyne CF. 3-D histomorphometry of the normal and early glaucomatous monkey optic nerve head: prelaminar neural tissues and cupping. *Invest Ophthalmol Vis Sci* 2007;48(11):5068-5084
- 24 Yang H, Downs JC, Girkin C, Sakata L, Bellezza A, Thompson H, Burgoyne CF. 3-D histomorphometry of the normal and early glaucomatous monkey optic nerve head: lamina cribrosa and peripapillary scleral position and thickness. *Invest Ophthalmol Vis Sci* 2007;48(10):4597-4607
- 25 Downs JC, Yang H, Girkin C, Sakata L, Bellezza A, Thompson H, Burgoyne CF. Three-dimensional histomorphometry of the normal and early glaucomatous monkey optic nerve head: neural canal and subarachnoid space architecture. *Invest Ophthalmol Vis Sci* 2007;48 (7): 3195-3208
- 26 Blumenthal EZ, Parikh RS, Pe'er J, Naik M, Kaliner E, Cohen MJ, Prabakaran S, Kogan M, Thomas R. Retinal nerve fibre layer imaging compared with histological measurements in a human eye. *Eye (Lond)* 2009;23(1):171-175
- 27 Mwanza JC, Oakley JD, Budenz DL, Anderson DR; Cirrus Optical Coherence Tomography Normative Database Study Group. Ability of Cirrus HD-OCT optic nerve head parameters to discriminate normal from glaucomatous eyes. *Ophthalmology* 2011;118(2):241-248
- 28 Quigley HA, Addicks EM. Regional differences in the structure of the lamina cribrosa and their relation to glaucomatous optic nerve damage. *Arch Ophthalmol* 1981;99(1):137-143
- 29 Manjunath V, Shah H, Fujimoto JG, Duker JS. Analysis of peripapillary atrophy using spectral domain optical coherence tomography. *Ophthalmology* 2011;118(3):531-536
- 30 Hayashi K, Tomidokoro A, Lee KY, Konno S, Saito H, Mayama C, Aihara M, Iwase A, Araie M. Spectral-domain optical coherence tomography of β -zone peripapillary atrophy: influence of myopia and glaucoma. *Invest Ophthalmol Vis Sci* 2012;53(3):1499-1505